Visual Abstract

Analyses of constraint factors to model damage accumulation ahead of the crack tip using the strip-yield model

Luiz Fernando Nazaré Marques
Federal University of South and Southeast of Pará, UNIFESSPA, Avenida dos Ipês s/n, Marabá, 68500-000, Brazil
lfernando@unifesspa.edu.br

Samuel Elias Ferreira, Jaime Tupiassú Pinho de Castro, Marco Antonio Meggiolaro, Luiz Fernando Martha
Pontifical Catholic University of Rio de Janeiro, PUC-Rio, R. Marquês de São Vicente 225, Rio de Janeiro, 22451-900, Brazil
ferreirase@hotmail.com, jtcastro@puc-rio.br, meggi@puc-rio.br, lfm@tecgraf.puc-rio.br

ABSTRACT. The combined strip-yield critical-damage model (SY-CDM) estimates the crack growth increments in a cycle-by-cycle basis through a gradual damage accumulation process ahead of the crack tip. So, it combines the strip-yield concepts with the cyclic damage accumulation routines. As well known, the strip-yield model (SYM) uses a plastic constraint factor α to increase the tensile flow stress S_F in the unbroken elements along the plastic zone (pz) during loading. This is done to consider the effects of the actually 3D stresses around the crack front, caused by plastic restrictions. In this work, a three-dimensional (3D) elastic-plastic (EP) finite element (FE) model is used to calculate plastic constraint factors α based on normalized EP normal-stress σ_{yy} inside the pz for a combination of geometries and load conditions in middle-crack tension M(T) specimen. The results indicate changes in α for different conditions. Thus, this factor variation behavior could be used to better estimate $da/dN \times \Delta K$ curves using SY-CDM model.

KEYWORDS. Incremental 3D finite elements elastoplastic calculations, plastic zone, constraint factor, fatigue crack growth, strip-yield model, damage accumulation.

OPEN ACCESS

Citation: Marques L.F.N., Ferreira S.E., Castro J.T.P., Meggiolaro M.A., Martha L.F., Analyses of constraint factors to model damage accumulation ahead of the crack tip using the strip-yield model, Frattura ed Integrità Strutturale, xx (2019) ww-zz.

Received: xx.yy.zzzz
Accepted: xx.yy.zzzz
Published: xx.yy.zzzz

INTRODUCTION

The plastic constraint factor α is an important parameter to predict and characterize fatigue crack growth (FCG) in cracked component. Several investigations have used three-dimensional (3D) elastic-plastic (EP) finite element analyses (FEA) to relate α to FCG and fracture behavior such as stable tearing, and unstable fracture [1-6]. The α level depends on the material stress-strain σ-ε properties, geometric and load parameters such as the component width-to-thickness W/B, the crack size-to-component width a/W, and the nominal stress-to-yield strength σ_n/S_Y ratios. From 3D EP FEA, equations describing α level have been proposed to be used on the strip-yield models (SYMs) [1-4].

Originally, the SYM uses a α to increase the tensile flow stress S_F in the unbroken elements along the plastic zone (pz) during loading. This is done to consider the effects of the 3D stresses around the crack front, due to plastic restrictions when the specimen is thick and cannot be assumed to work under plane stress *pl*-σ. Fig. 1 shows the crack surface displacements and the stress distributions around the crack tip [7]. It is formed by: 1) a linear elastic region containing a fictitious crack of half-length a + pz; (2) a plastic region of length pz and (3) a residual plastic deformation region along the crack surface. The pz is discretized in a series of rigid-perfectly plastic 1D bar elements, which are assumed to yield at the flow strength of the material.

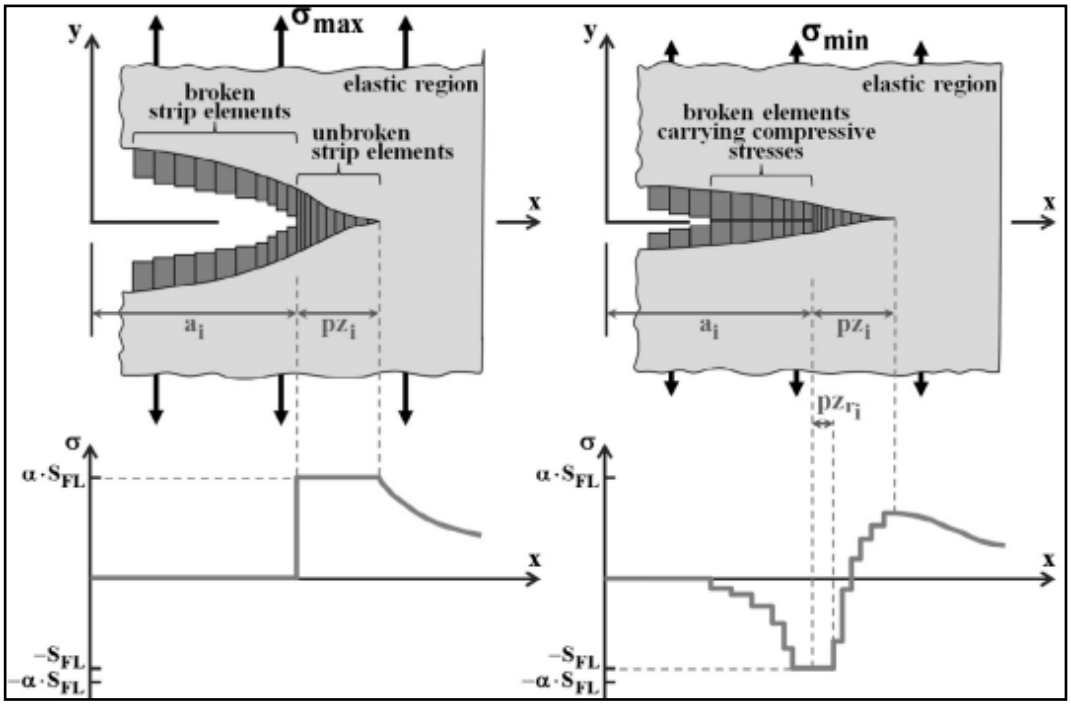

Figure 1: Crack surface displacements and stress distribution along the crack line at the maximum and minimum applied stresses [7].

The α parameter should vary from $\alpha = 1$ for *pl*-σ to up to $\alpha = 1/(1-2\nu) \approx 3$ for plane strain *pl*-ε limit conditions, where ν is Poisson's coefficient. The factor α is used to accommodate, in the SYM, a more general case of stress state improving the simulation of measured $da/dN \times \Delta K$ curves.

There is a number of detailed 3D EP FE studies to characterize α based on geometric and load conditions [1-4]. This series of studies presents several versions of α and its evolutions along time. The simplest plastic constraint factors α are based on the normal, tangential, and hydrostatic-stresses along the crack front [1]. The normal-stress α is defined as the ratio of the normal stress-to-yield strength (σ_{yy}/S_Y) along the crack front, Eq. 1. Likewise, the tangential-stress γ is defined as the ratio of the tangential stress-to-yield strength (σ_{xx}/S_Y) and the hydrostatic-stress χ is defined as the ratio of the hydrostatic stress-to-yield strength (σ_m/S_Y). Changes in these local factors along the crack front with different, a/W, W/B and σ_n/S_Y ratios are presented. In the same work, a global constraint factor α_g is defined as the average normal-stress-to-yield strength ratio acting over the yielded elements on the untracked ligament, Eq. 2.

$$\alpha \ \ z = \frac{\sigma_{yy}}{S_Y} \qquad \text{Eq. 1}$$

$$\alpha_g = \frac{1}{A_T} \sum_{n=1}^{Ele} \left(\frac{\sigma_{yy}}{S_Y} \right)_n \cdot A_n \qquad \text{Eq. 2}$$

where A, is the projected area on the uncracked ligament of a yielded element n, σ_{yy}/S_Y is the normalized normal-stress, and A_T is the total projected area for all elements *Ele* yielded.

In other work [2], 3D EP FE analyses are performed to study the stresses and deformations around crack fronts in three specimen types: middle-crack tension M(T), double-edge-crack tension DE(T) and single-edge-crack bend SE(B). All simulations are made using an elastic-perfectly plastic material. The α_g is defined for using with a SYM. Using this combination α_g-SYM, both the pz sizes and crack tip displacements for the M(T) cracked component agreed well with 3D FE results.

Further, two new factors are proposed to evaluated the stresses and deformations around semi elliptical surface cracks in a plate subjected to tension and bending loads [3]. Both constraint factors are similar to the α_g, developed by Newman et al [1, 2]. The hyper-local normal-stress constraint factor α_h is the average of the normal-stress acting along a ray perpendicular to the crack front of the yielded elements. This factor is defined as

$$\alpha_h(\phi) = \frac{1}{A_r(\phi)} \sum_{n=1}^{Ele(\phi)} \left(\frac{\sigma_{yy}}{S_Y} \right)_n \cdot A_n \qquad \text{Eq. 3}$$

where $A_r(\phi)$ is the total projected area for all yielded elements along a given ray $Ele(\phi)$.

For comparison, a hyper-local hydrostatic-stress constraint is given by

$$\chi_h(\phi) = \frac{1}{A_r(\phi)} \sum_{n=1}^{Ele(\phi)} \left(\frac{\sigma_m}{S_Y} \right)_n \cdot A_n \qquad \text{Eq. 4}$$

where σ_m is the hydrostatic-stress given by $(\sigma_{xx} + \sigma_{yy} + \sigma_{zz})/3$.

Both hyper-local constraint factors show the same trends but χ_h at lower magnitudes. Thus, they could be used to describe the surface crack constraint behavior as well. For comparison, the α_g for a through-the-thickness crack under pure plane strain bending is measured and found to be about 2.7 [2], a higher value than the results for α_h and χ_h.

The more evolved constraint factor $\alpha(\phi)$ are investigated in [4]. It is a modified version of the α_h [3], which is an evolution of the α_g [1]. The previous assessments are based on an elastic perfectly plastic material [1-3]. In this new version, a single analysis is conducted on a tension model using the engineering notation $\varepsilon = \sigma/E + (\sigma/H)^{1/h}$, where E is the modulus of elasticity, H and h are the Ramberg-Osgood parameters. The calculation of individual element areas is eliminated entirely by defining constraint as the normal-stress-to-yield strength ratio acting along a line or path, Fig. 2. This new constraint factor is defined as

$$\alpha(\phi) = \frac{1}{S(\phi)} \int_0^{S(\phi)} \left(\frac{\sigma_{yy}}{S_Y} \right) ds \qquad \text{Eq. 5}$$

where $S(\phi)$ defines the arc length of a hyperbolic path originating and perpendicular to the crack front at ϕ and terminating at the perimeter of the pz and σ_{yy}/S_Y is the normalized normal-stress component interpolated onto the defined path at location s.

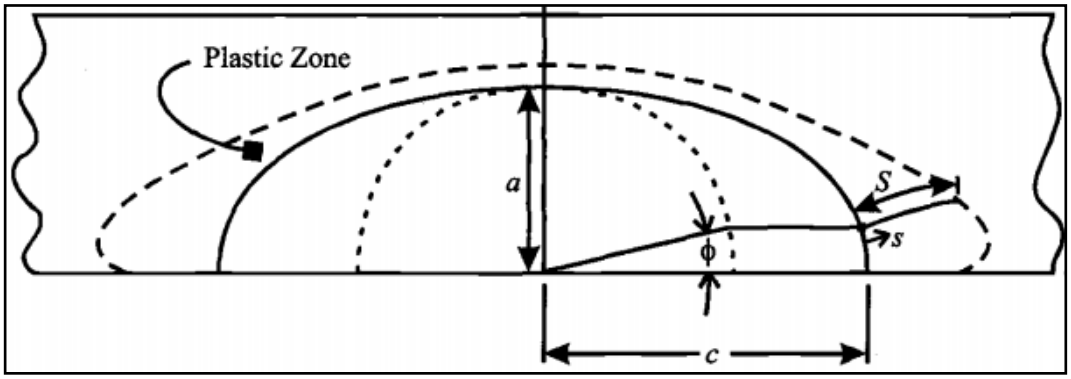

Figure 2: Normal stress constraint factor for surface crack [4].

All equations describing the plastic constraint factor α level may be used on the new combined strip-yield critical-damage model (SY-CDM). This approach estimates the crack growth increments in a cycle-by-cycle basis through a gradual damage accumulation process ahead of the crack tip. So, it combines the strip-yield concepts with the cyclic damage accumulation routines well described elsewhere [8, 9].
In this work, a constitutive multilinear isotropic hardening model is used to numerically estimate the 3D EP frontiers of the monotonic pzs in terms of the Mises equivalent strain ε_{eq}, as well as the normalized EP normal-stress σ_{yy}/S_Y distributions inside them to calculate the plastic constraint factors α for a combination of geometries and load conditions. Finally, the results of these factors are evaluated. Then, proposed how this factor variation behavior could be used to better estimate da/dN×ΔK curves using SY-CDM model.

Finite Element Analyses

All numerical simulations are performed considering only 1/8 of the modeled M(T) specimen due to their symmetries. The procedure involves two calculation steps. Firstly, the global model without considering a denser refinement mesh is solving. Then, the submodel that contains the pz with a much more refined mesh.

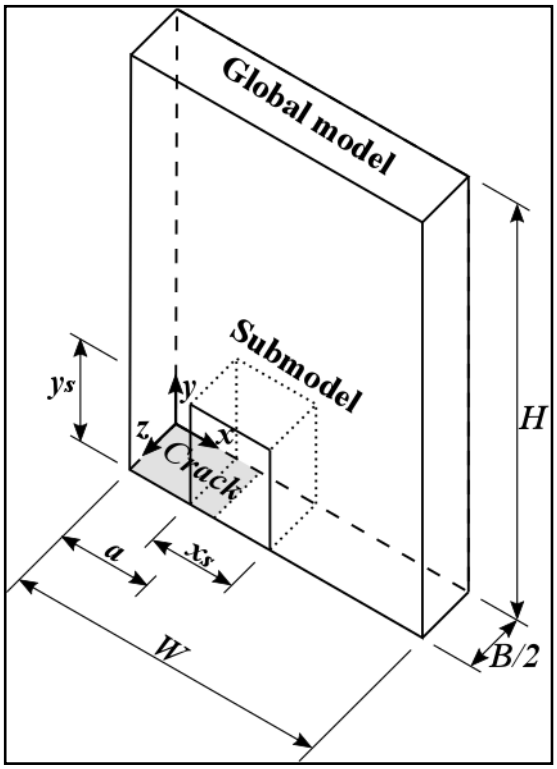

Figure 3: Some characteristics of the global models and sub-models [6].

Quadratic elements (3D SOLID186) are used in these FE simulations, and only the fractions of the volumes corresponding to their plastified Gauss integration points are counted as part of the 3D pz around the crack fronts. So, the smallest unit of volume treated in the pz models became 1/8 of the volume of the element [6].

For the traditional specimen selected for this study, there are well-known expressions for Stress Intensity Factor (SIF) in mode I K_I available in the literature: $K_I = P/(B\sqrt{W})f(a/W)_{Specimen}$, where $f(a/W)_{Specimen}$ is a geometry function that depends on the crack size-to-specimen width a/W ratio. The Eq. 6 presents the function for the cracked component M(T) [10] used in all numerical simulations.

$$f\left(\frac{a}{W}\right)_{M(T)} = \sqrt{\left(\frac{\pi a}{4W}\right)\sec\left(\frac{\pi a}{2W}\right)}\left[1-0.025\left(\frac{a}{W}\right)^2+0.06\left(\frac{a}{W}\right)^4\right] \quad \text{Eq. 6}$$

Numerical validation

To validate the 3D EP FE model, a comparison is made to classic 3D results taken from Newman et. al [1, 2] for M(T) specimen. The numerical simulation is performed considering only 1/8 of the modeled M(T) due to its symmetries, using W = 40mm, $H = 2W$, a/W = 0.5, and W/B = 8. The material was assumed to be elastic perfectly plastic with E = 71.5GPa, S_Y = 500MPa and ν = 0.3. The applied normalized SIF is $K_I/(S_Y\sqrt{W})$ = 0.33. The simplest plastic constraint factors $\alpha = \sigma_{yy}/S_Y$ obtained only for W/B = 8 are show in Fig. 4. In addition, two global normal-stress constraint factors, $\alpha_{mean} = (\sigma_{yy}/S_Y)_{mean}$ = 2.63 and α_g = 1.72, are presented on the same graph. Newman's results are also illustrated for three W/B ratios to make comparisons [1].

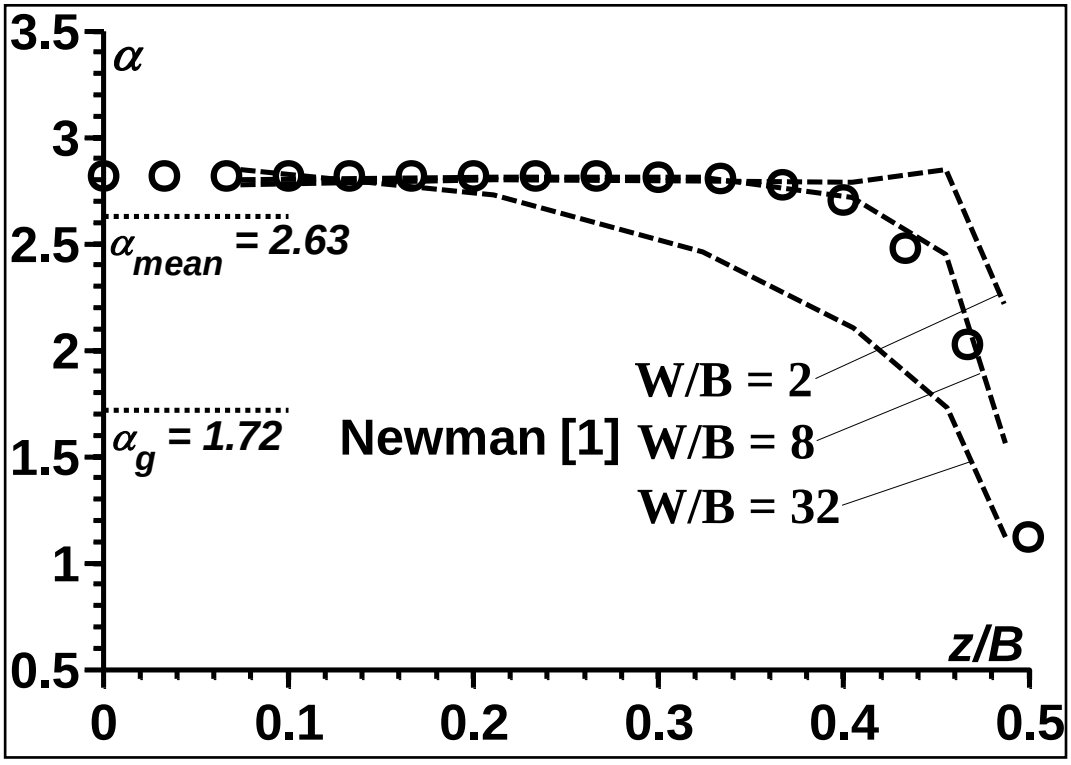

Figure 4: Local and global normal-stress constraint factors along the crack front.

GLOBAL CONSTRAINT FACTOR VARIATION

Based on the plastic constraint factor α approach and its evolution [1-4], an evaluation of α is made this work. The factor α should vary with changes in the component geometries, material and loading conditions. To check so, for a given K_I = 25MPa$\sqrt{m}$, the geometry parameter represented by crack length-to-component width (a/W = 0.15, 0.20 and 0.25) and

loading condition represented by nominal applied stress-to-yield strength (σ_n/S_Y = 0.4, 0.5 and 0.6) ratios are simulated. The M(T) component thickness-to-component width is B/W = 8. The mechanical properties are given in Tab. 1 [11], and the true σ-ε curve used in the 3D EP FE models is shown in Fig. 5.

Table 1: Material and properties [11].

Material	E (GPa)	ν ( )	S_U (MPa)	S_Y (MPa)	EL (%)	RA (%)	H (MPa)	h ( )
7075-T6	72	0.33	576	489	17	11	793	0.09

The constraint factor α investigated in this work is a modified version available in the literature [4]. The α constraint variations around a straight through crack in M(T) specimen is defined by

$$\alpha(z) = \frac{1}{X(z)} \sum_{n=1}^{Gp(z)} \left(\frac{\sigma_{yy}}{S_Y} \right)_n \cdot X_n \qquad \text{Eq. 7}$$

where X_n is the length of the projected path line from and normal to the crack front at z up to the perimeter of the plastic zone, σ_{yy}/S_Y is the normalized stress component onto the defined path line at location z for Gauss point n, and $X(z)$ is the total length of the projected path line for all yielded Gauss points along a given perimeter of the pz $Gp(z)$.

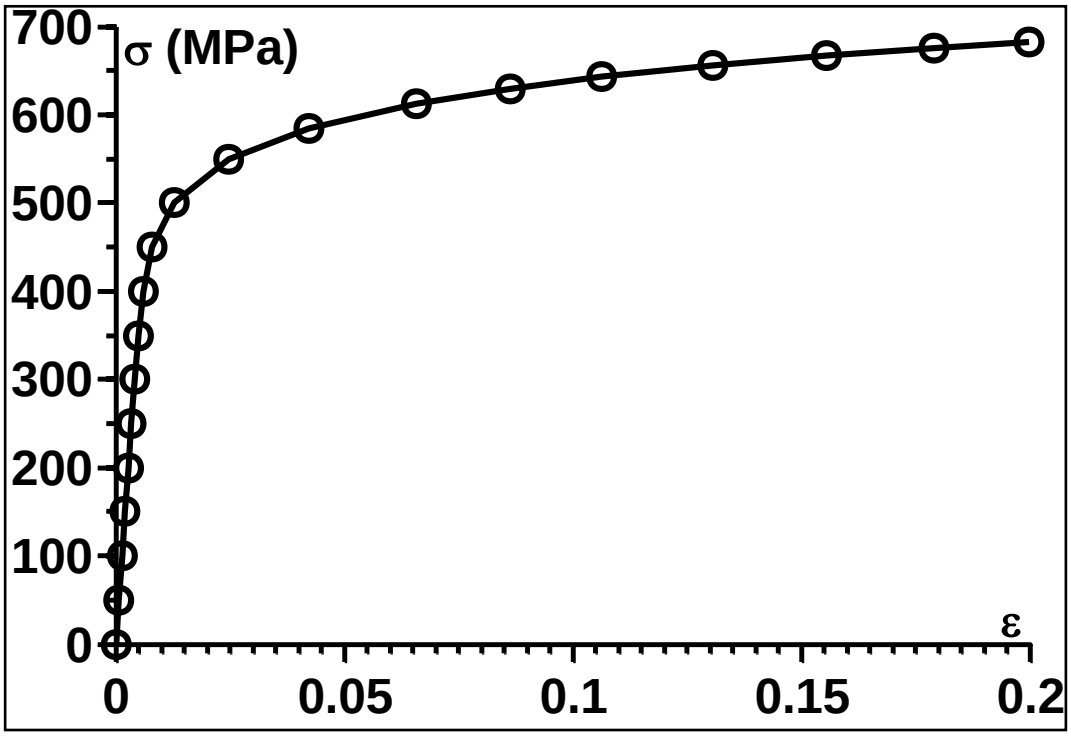

Figure 5: The true stress-strain curve of the studied 7075-T6 aluminum alloy.

Fig. 6 shows the middle tension M(T) cracked component modeled in this study and details of the pz area ahead of the crack front used to calculated α.

Fig. 7 illustrates the plastic constraint factors along the crack front for a K_I = 25MPa$\sqrt{m}$, geometries and loading conditions adopted in this study. These constraint factors are calculated by Eq. 7. Tab. 2 presents the average α_{mean} variations for each condition. For the M(T) cracked component, the plastic constraint factor decrease as the crack length (a/W) and load condition (σ_n/S_Y) decrease.

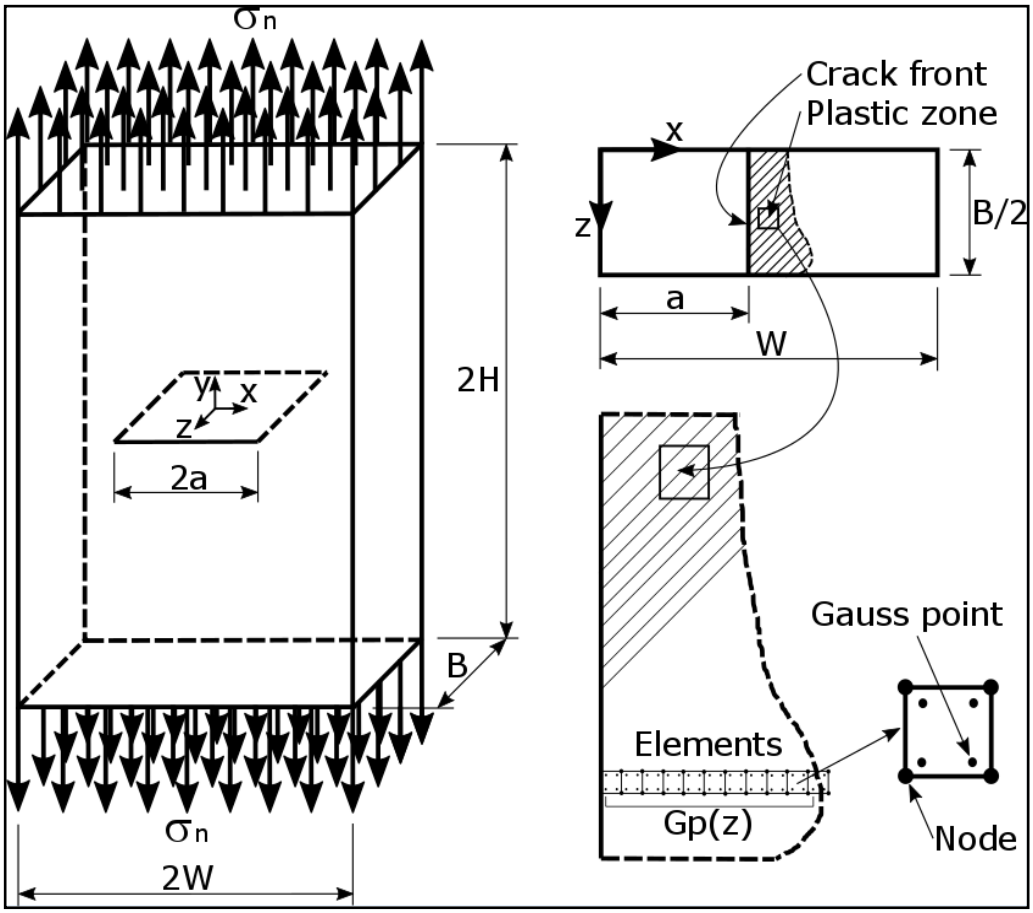

Figure 6: M(T) specimen geometry and details of the perimeter of the plastic zone.

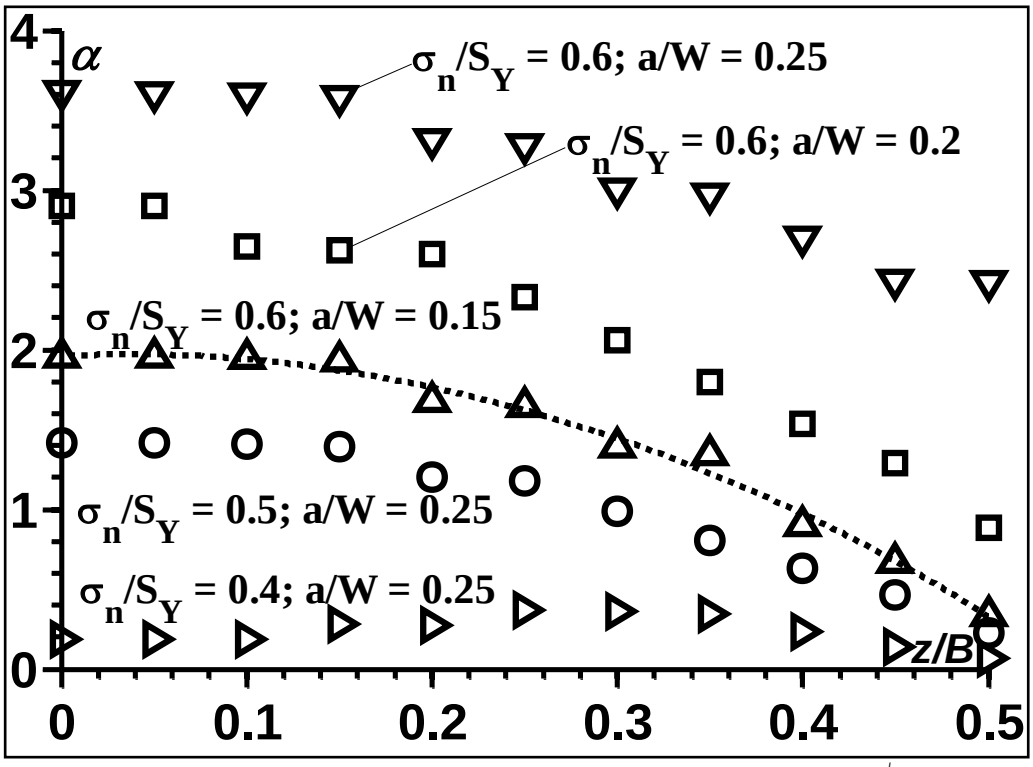

Figure 7: Plastic constraint factors along the crack front for a K_I = 25MPa√m.

Changes in σ_n/S_Y may affect the pz sizes, as studied elsewhere [12]. Whether the plastic constraint factor is also modified by σ_n/S_Y, thus the prediction and characterization of fatigue crack growth (FCG) in cracked component may be affected as well.

Table 2: Average plastic constraint factor α_{mean} for geometries and loading conditions.

a/W	σ_n/S_Y		
	0.4	0.5	0.6
0.15	-	-	1.43
0.20	-	-	2.14
0.25	0.24	1.01	3.14

CONCLUSIONS

In this work a 3D elastoplastic finite element analyses have been used to compute the plastic constraint variations around a straight through crack in middle tension cracked component. First, the numerical results reproduced well the classic 3D results taken from Newman for the same M(T) specimen. Based on plastic constraint factos along the crack front, this study suggests that predictions and characterizations of fatigue crack growth in cracked component may be affected by geometries and load conditions σ_n/S_Y. Using this definition to quantify the plastic constraint factor, it is possible to calibrate these factors as a function of geometries and load conditions.

ACKNOWLEDGEMENTS

Luiz Fernando Nazaré Marques would like to gratefully acknowledge the support received from PUC-Rio.

REFERENCES

[1] Newman, J. C. JR., Bigelow, C. A. and Shivakumar, K. N., "Three-Dimensional Elastic-Plastic Finite-Element Analyses of Constraint Variations in Cracked Bodies". Engineering Fracture Mechanics Vol.46, No. 1, 1993, pp, 1-3.
[2] Newman, J. C., Jr., Crews, J. H., Jr., Bigelow, C. A., and Dawicke, D. S., "Variations of a Global Constraint Factor in Cracked Bodies Under Tension and Bending Loads," Constraint Effects in Fracture Theory and Applications: Second Volume, ASTM STP 1244, M. Kirk and A. Bakker, Eds., American Society for Testing and Materials, 1995, pp. 2142.
[3] Newman, J. C., Jr., Reuter, W. G., and Aveline, C. R., Jr., "Stress and Fracture Analyses of Semi-Elliptical Surface Cracks," Fatigue and Fracture Mechanics: 30th Volume, ASTM STP 1360, P. C. Paris and K. L. Jerina, Eds., American Society for Testing and Materials, West Conshohocken, PA, 2000, pp. 403-423.
[4] Aveline, C. R., Jr. and Daniewicz, S. R., "Variations of Constraint and Plastic Zone Size in Surface-Cracked Plates Under Tension or Bending Loads," Fatigue and Fracture Mechanics: 31st Volume, ASTM STP 1389, G. R. Halford and J. P. Gallagher, Eds., American Society for Testing and Materials, West Conshohocken, PA, 2000, pp. 206-220.
[5] C. She, W. Guo. The out-of-plane constraint of mixed-modecracks in thin elastic plates. Int J Solids Struct 44 (2007) 3021–3034.
[6] Marques, L. F. N. et al., On the estimation of the elastoplastic work needed to initiate crack tearing. Theoretical and Applied Fracture Mechanics 101 (2019) 80–91.
[7] Newman Jr JC. A crack-closure model for predicting fatigue crack growth under aircraft spectrum loading. Methods Models Predict Fatigue Crack Growth Under Random Load, ASTM STP 1981;748:53–84.
[8] Ferreira, S.E. et al., Using the strip-yield mechanics to model fatigue crack growth by damage accumulation ahead of th.e crack tip. International Journal of Fatigue 103 (2017) 557–575.
[9] Ferreira, S.E., IJF (2018), https://doi.org/10.1016/j.ijfatigue.2018.03.001.
[10] Durán JAR, Castro JTP, Payão Filho JC. Fatigue crack propagation prediction by cyclic plasticity damage accumulation models. Fatigue Fract Eng Mater Struct 2003;26:137–50.
[11] T. L. Anderson, Fracture Mechanics: Fundamentas and Aplications, third ed., Taylor & Francis, (2005).
[12] Souza, R.A., Castro, J.T.P., Lopes, A.A.O., Martha, L.F., "On improved crack tip plastic zone estimates based on T-stress and on complete stress fields". Fatigue FractEng Mater Struct36 (2013) 25-38.